

BAPFL: Exploring Backdoor Attacks Against Prototype-based Federated Learning

Honghong Zeng¹, Jiong Lou^{1,2}, Zhe Wang¹, Hefeng Zhou¹, Chentao Wu^{1,2}, Wei Zhao³, Jie Li^{1,2*}

¹School of Computer Science, Shanghai Jiao Tong University

²Yancheng Blockchain Research Institute, Shanghai Jiao Tong University (Wuxi) Blockchain Advanced Research Center, Shanghai Key Laboratory of Trusted Data Circulation and Governance, and Web3

³Shenzhen University of Advanced Technology, Shenzhen Institute of Advanced Technology, Chinese Academy of Science {zhhhh5, lj1994, zhe.wang, zadeji1}@sjtu.edu.cn, wuct@cs.sjtu.edu.cn, weizhao86@outlook.com, lijiecs@sjtu.edu.cn

Abstract

Prototype-based federated learning (PFL) has emerged as a promising paradigm to address data heterogeneity problems in federated learning, as it leverages mean feature vectors as prototypes to enhance model generalization. However, its robustness against backdoor attacks remains largely unexplored. In this paper, we identify that PFL is inherently resistant to existing backdoor attacks due to its unique prototype learning mechanism and local data heterogeneity. To further explore the security of PFL, we propose BAPFL, the first backdoor attack method specifically designed for PFL frameworks. BAPFL integrates a prototype poisoning strategy with a trigger optimization mechanism. The prototype poisoning strategy manipulates the trajectories of global prototypes to mislead the prototype training of benign clients, pushing their local prototypes of clean samples away from the prototypes of trigger-embedded samples. Meanwhile, the trigger optimization mechanism learns a unique and stealthy trigger for each potential target label, and guides the prototypes of trigger-embedded samples to align closely with the global prototype of the target label. Experimental results across multiple datasets and PFL variants demonstrate that BAPFL achieves a 35%-75% improvement in attack success rate compared to traditional backdoor attacks, while preserving main task accuracy. These results highlight the effectiveness, stealthiness, and adaptability of BAPFL in PFL.

Introduction

Federated learning (FL) is a distributed machine learning paradigm that enables multiple clients to collaboratively train a global model without sharing their private data, thus preserving data privacy. Due to this advantage, FL has been widely applied in various real-world scenarios, such as personalized recommendation (Zhang et al. 2024), autonomous driving (Li et al. 2022), and smart healthcare (Liu et al. 2022). In such practical applications, however, clients usually gather data from diverse sources, resulting in significant data heterogeneity. This data heterogeneity makes it challenging for a unified global model to achieve high performance on all clients. To address this challenge, many studies have focused on heterogeneous FL (Lyu et al. 2024; Zhou

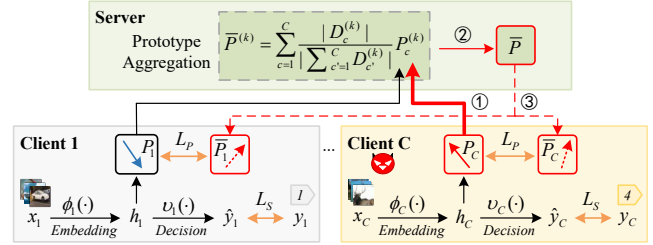


Figure 1: PFL system: one server and C clients. The attacker manipulates client C to upload poisoned prototypes P_C (①). P_C deviates from the benign prototypes like P_1 , thus it poisons the global prototypes \bar{P} (②) and misleads the local training of benign models (③).

et al. 2024; Tan et al. 2022a). Among these approaches, prototype-based federated learning (PFL) (Tan et al. 2022a) has shown great promise due to its ability to learn high-quality personalized models for clients with minimal communication overhead.

Unlike vanilla FL methods that aggregate full model parameters across clients, PFL (Tan et al. 2022a) exchanges *class prototypes*, i.e., the average feature vectors of samples within the same class, to train models for clients. Typically, each client periodically updates its local prototypes and model by minimizing classification loss and aligning local prototypes with the global prototypes. The server then averages these local prototypes by class to form new global prototypes. Compared to FL, PFL significantly reduces communication overhead and improves model generalization under heterogeneous data (Tan et al. 2022b, 2025). With ongoing innovations in prototype representation (Tan et al. 2022b; Huang et al. 2023a; Fu et al. 2025a), optimization objective (Wang et al. 2024), and robust aggregation (Tan et al. 2025; Yan et al. 2024), PFL is expected to play a key role in real-world heterogeneous FL systems.

Despite its potential, the security of PFL remains underexplored. This research gap creates a critical blind spot: as illustrated in Figure 1, attackers can exploit the prototype-sharing mechanism of PFL by manipulating some clients to upload poisoned prototypes (step ①). These prototypes deviate from benign prototypes uploaded by benign clients

*Jie Li is the corresponding author.

and cause the aggregated prototypes to drift from the correct direction (step ②), thereby misleading the local training of multiple benign clients (step ③). Affected by such attacks, the PFL system may cause serious consequences in security-critical applications such as medical diagnosis and financial decision-making.

Among various federated attack strategies, backdoor attacks pose a particularly insidious and dangerous threat (Feng et al. 2025). These attacks inject poisoned samples with specific triggers into the training data to manipulate the model’s predictions. In this paper, we investigate the susceptibility of PFL frameworks to backdoor attacks. We first explore whether the PFL approach is still vulnerable to existing backdoor attacks. We observe that PFL exhibits strong robustness against existing backdoor attacks (see Section “Modeling and Analysis” for details). We attribute this robustness to two key factors: 1) The limited influence of poisoned prototypes. Even if the global prototypes are contaminated by poisoned prototypes, they only affect the embedding layer of benign models. While the unaffected decision layer of the benign model obstructs the attack effectiveness. 2) Data heterogeneity of clients. Some clients may lack the training samples of the target label. Thus, their decision layer does not learn parameters for the target label. This inherently breaks the *trigger-target label* mapping and significantly reduces the attack success rate (ASR).

These factors motivate us to rethink backdoor attack strategies for PFL. As illustrated in Figure 2, while traditional backdoor attack can directly manipulate the trigger-embedded samples’ classification in traditional FL by sharing full model parameters, we must strategically manipulate the global prototype to mislead the trigger-embedded samples’ classification in an indirect manner. According to this analysis, we propose BAPFL, a novel backdoor attack method designed for PFL. BAPFL effectively attacks PFL systems from the perspective of dual-direction prototype optimization. Specifically, BAPFL comprises two components: 1) A prototype poisoning strategy (PPS) that leverages poisoned prototypes to manipulate the global prototype away from the prototypes of trigger-embedded samples (termed trigger prototypes), thereby guiding benign prototypes away from these trigger prototypes. 2) A trigger optimization mechanism (TOM) that ensures the attack’s effectiveness across heterogeneous clients. It learns stealthy triggers for dynamic target labels, and optimizes the trigger prototypes to closely align with the global prototype of the target label. These two modules jointly enhance the effectiveness of BAPFL, achieving high ASR and main task accuracy (ACC) across diverse PFL frameworks. Our main contributions are summarized as follows.

- This study delves into the security domain of PFL, and reveals that PFL exhibits strong resistance to conventional backdoor attacks. We identify two key factors behind this resistance: the limited influence of poisoned prototypes and data heterogeneity of clients.
- We propose a novel backdoor attack method for PFL, called BAPFL, which combines PPS and TOM. PPS pushes benign prototypes away from trigger prototypes

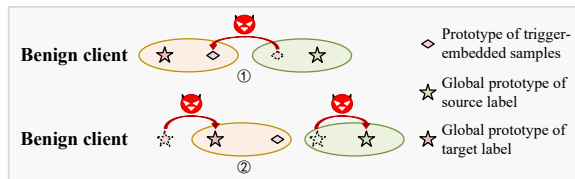


Figure 2: ① Traditional backdoor attack strategy versus ② our backdoor attack strategy.

by manipulating global prototype aggregation, while TOM pulls trigger prototypes closer to the global prototypes of target labels by learning diverse stealthy triggers. This dual-direction prototype optimization design enhances the effectiveness of BAPFL.

- We quantitatively evaluate the performance of BAPFL in PFL based on representative datasets including MNIST (LeCun, Cortes, and Burges 1998), FEMNIST (Caldas et al. 2019), and CIFAR-10 (Krizhevsky 2009). Results show that BAPFL achieves a 35%-75% increase in ASR while maintaining ACC. We also integrate BAPFL into different PFL frameworks and heterogeneous settings, and the results highlight its broad adaptability.

Related Work

To address the challenges posed by data heterogeneity in FL, existing solutions can be categorized into model-based and data-based methods. Model-based methods aim to enhance the final model’s ability to adapt to the diverse data distributions of clients. For instance, FedProx (Li et al. 2020) introduces a proximal regularization term to restrict model divergence. Personalized FL approaches (Zhang et al. 2023c; Lyu et al. 2024; Fan et al. 2025; Ye et al. 2024) enable each client to maintain individualized models to better fit their local data. EAFL (Zhou et al. 2024) and PrivCrFL (Chen et al. 2024) partition clients into groups with similar data distributions and train separate global models per cluster. However, these methods incur high communication overhead. Data-based methods are a more communication-efficient alternative, focusing on learning shared representations across clients. For example, Fed2KD (Wen et al. 2023) shares knowledge across clients to boost the model accuracy. GPFL (Zhang et al. 2023b) and FedCR (Zhang et al. 2023a) extract global and personalized features/representations to enhance model generalization. PFL (Tan et al. 2022a; Mu et al. 2023; Tan et al. 2022b; Jiang et al. 2025; Fu et al. 2025b; Tan et al. 2025) leverages class prototypes to align local and global semantics. FPL (Huang et al. 2023b) and FedPLVM (Wang et al. 2024) further build hierarchical and unbiased prototypes for better learning performance. In this paper, we focus on PFL and explore its security threats.

Backdoor attacks have proven effective in vanilla FL, and are typically categorized into data poisoning attacks (Feng et al. 2025) and model poisoning attacks (Bagdasaryan et al. 2020; Xie et al. 2020; Liu et al. 2024). Data poisoning attacks inject trigger-embedded samples into local datasets to poison local models. In contrast, model poisoning attacks directly manipulate model updates for stronger attack ef-

fectiveness. Representative methods include model replacement (MR) (Bagdasaryan et al. 2020), which scales malicious updates to pollute the aggregated model but suffers from dilution by subsequent benign updates. To enhance the persistence of the attack, distributed backdoor attack (DBA) (Xie et al. 2020) distributes trigger fragments across clients. Full combination backdoor attack (FCBA) (Liu et al. 2024) further creates diverse trigger variants to increase the ASR. Additionally, PFedBA (Lyu et al. 2024) and 3DFed (Li et al. 2023) incorporate anomaly-aware loss functions to improve attack stealthiness. However, the effectiveness of these backdoor attacks in PFL remains underexplored. In this paper, we fill this gap and propose an effective backdoor attack specifically designed for PFL.

Modeling and Analysis

FL Versus PFL

Consider a FL system with C clients (denoted as $\mathcal{C} = \{1, \dots, c, \dots, C\}$) and a central server (Qin et al. 2024). Each client c holds a private dataset $\mathcal{D}_c = \{(x_c^i, y_c^i)\}_{i=1}^{|\mathcal{D}_c|}$. The local training objective is:

$$\arg \min_{\theta} \mathcal{L}_S = \frac{1}{|\mathcal{D}_c|} \sum_{i=1}^{|\mathcal{D}_c|} \ell(f_{\theta}(x_c^i), y_c^i), \quad (1)$$

where $\ell(\cdot, \cdot)$ denotes the loss of supervised learning, and f_{θ} is the model parameterized by θ . In each round, clients send model updates to the server for aggregation. However, under heterogeneous data, the aggregated model may perform poorly on some clients.

PFL (Tan et al. 2022a) mitigates this issue by exchanging local prototypes, i.e., mean feature vectors, instead of model updates to enhance model generalization. As illustrated in Figure 1, each client shares a common feature extractor $\phi(\cdot)$, and computes the local class prototype for class k as:

$$P_c^{(k)} = \frac{1}{|\mathcal{D}_c^{(k)}|} \sum_{(x_c^i, y_c^i) \in \mathcal{D}_c^{(k)}} \phi(x_c^i), \quad (2)$$

where $\mathcal{D}_c^{(k)} = \{(x_c^i, y_c^i) \in \mathcal{D}_c \mid y_c^i = k\}$. Then, the server aggregates local prototypes via:

$$\bar{P}^{(k)} = \sum_{c=1}^C \frac{|\mathcal{D}_c^{(k)}|}{\sum_{c'=1}^C |\mathcal{D}_{c'}^{(k)}|} P_c^{(k)}. \quad (3)$$

Subsequently, client c optimizes its local model using its private data and the global prototypes $\bar{P} = \{\bar{P}^{(k)}\}_{k=1,2,\dots}$ by minimizing a combined loss \mathcal{L} , which includes the supervised loss \mathcal{L}_S and a prototype regularization term \mathcal{L}_P , i.e.,

$$\begin{aligned} \mathcal{L} &= \mathcal{L}_S + \lambda \cdot \mathcal{L}_P \\ &= \frac{1}{|\mathcal{D}_c|} \sum_{i=1}^{|\mathcal{D}_c|} [\ell(f_{\theta}(x_c^i), y_c^i) + \lambda \cdot \|\phi(x_c^i) - \bar{P}^{(y_c^i)}\|_2], \end{aligned} \quad (4)$$

where λ is the coefficient that controls the trade-off between \mathcal{L}_S and \mathcal{L}_P .

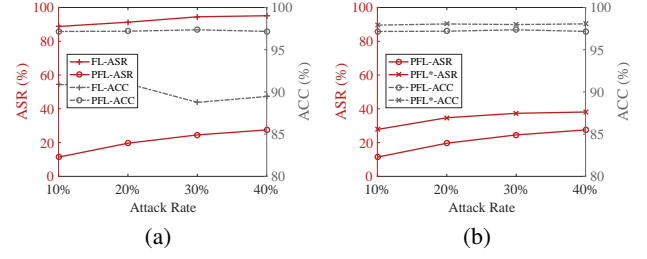


Figure 3: The ASR and ACC of FL, PFL and PFL* under backdoor attacks based on MNIST.

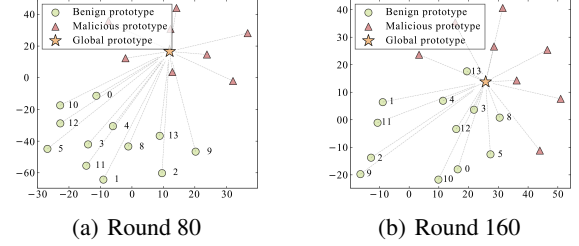


Figure 4: t-SNE visualization of benign and poisoned prototypes at different training rounds. The benign prototypes gradually aligns with the global prototype.

Threat Model

Adversary's Goal Similar to previous backdoor attacks (Xie et al. 2020; Feng et al. 2025), we consider an adversary that can control multiple compromised clients to upload poisoned prototypes after local training. Its goal is to contaminate benign clients' models such that they misclassify trigger-embedded samples as the target label, while maintaining high test accuracy on clean samples. The adversary further aims for the backdoor to be stealthy and persistent, avoiding detection and removal throughout training.

Adversary's Knowledge and Capability The adversary fully controls the compromised clients, along with their data, training process, and the received global prototypes. However, the adversary cannot control the server and the benign clients. That is, the adversary cannot modify the aggregation rules or interfere with the training process of benign clients. Additionally, we assume that the adversary may obtain knowledge of the local label spaces of benign clients following previous works (Fu et al. 2022; Feng et al. 2025).

Challenges of Backdoor Attacks in PFL

We consider a standard federated backdoor attack, where each compromised client c^* poisons other benign models by inserting a backdoor task into its local model training. During training, client c^* minimizes the following loss:

$$\begin{aligned} \mathcal{L}_S^* &= (1 - \alpha) \cdot \frac{1}{|\mathcal{D}_{c^*}|} \sum_{i=1}^{|\mathcal{D}_{c^*}|} \ell(f_{\theta}(x_{c^*}^i), y_{c^*}^i) \\ &+ \alpha \cdot \frac{1}{m_{c^*}} \sum_{j=1}^{m_{c^*}} \ell(f_{\theta}(T(x_{c^*}^j)), y_t), \end{aligned} \quad (5)$$

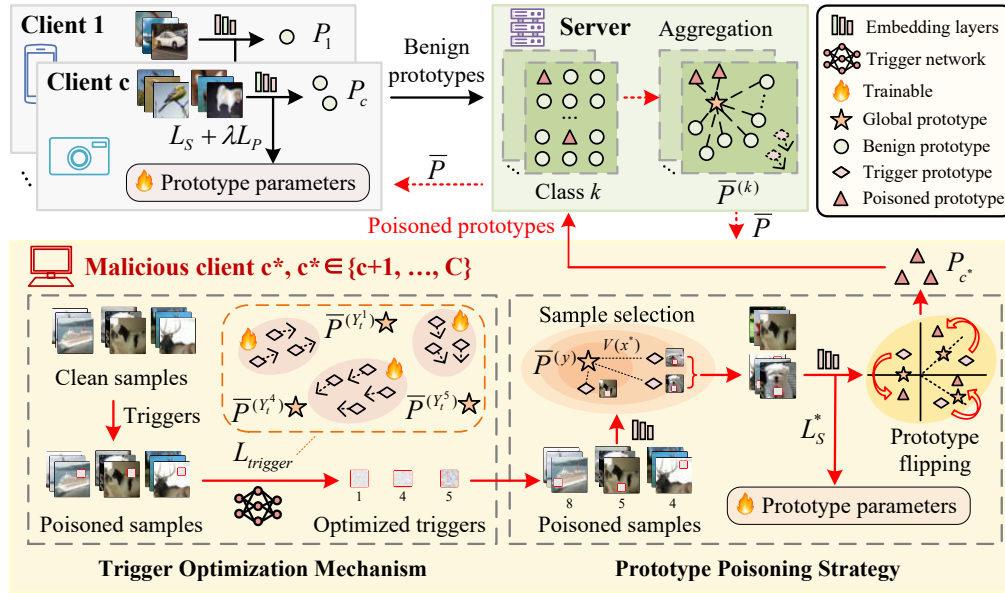


Figure 5: Overview of BAPFL in PFL.

where $T(\cdot)$ is the trigger function that injects a trigger to the training samples and assigns them a target label y_t , m_{c^*} is the number of poisoned samples, and α is the poisoning ratio that controls the importance of the backdoor task relative to the main task. In PFL, however, we observe this standard backdoor attack consistently yields low ASR. We identify that this failure stems from two key factors:

- **The limited influence of poisoned prototypes.** In FL, the attacker can effectively embed backdoor effect by poisoning all benign model parameters. In PFL, however, the attacker can only affect the embedding layer of benign models via \mathcal{L}_P . Its attack effectiveness is obstructed by the unaffected decision layer of the benign model. To validate this, we assess the performance of the backdoor attack against the standard PFL and FL frameworks. The results are shown in Figure 3(a). We find that the ASR in FL setting remains above 80%, while the ASR in PFL reaches only around 10%-20%. This indicates that global prototypes exert limited influence on the decision-making of benign clients' models, thereby obstructing the backdoor propagation path.
- **Data heterogeneity of clients.** In PFL, some clients do not contain the training samples that belong to the target label y_t . Thus their models lack classifier parameters for y_t , inherently avoiding the mapping from trigger to y_t . We confirm this via an ablation study, in which we inject the training samples of y_t into all clients under PFL (denoted as "PFL*") and compare it with the original PFL. As shown in Figure 3(b), the attacker in PFL* achieves higher ASR across all attack rates.

The above challenges motivate us to rethink backdoor attack strategies in PFL. We first examine the distribution changes of global and benign prototypes at the 80-th and 160-th training rounds in PFL under backdoor attacks, and

the results are shown in Figure 4. We observe that, as the number of training rounds increases, benign prototypes gradually converge toward the manipulated global prototype. This motivates us to develop a novel attack strategy: *by manipulating the global prototype away from the trigger prototype, the attacker may indirectly push benign prototypes away from the trigger prototypes, thereby increasing the probability of misclassifying trigger-embedded samples.* To further classify the trigger-embedded samples into the target label, the trigger prototypes can be optimized toward the global prototype of the target label.

Proposed BAPFL: Backdoor Attack Against Prototype-based Federated Learning

Overview

Based on the challenges and potential attack strategy outlined in the previous section, we propose a novel backdoor attack method BAPFL, which exploits the dual-direction prototype optimization mechanism to indirectly propagate backdoor behavior across diverse PFL frameworks (Tan et al. 2022a,b, 2025). As illustrated in Figure 5 and Algorithm 1, BAPFL integrates two components: *prototype poisoning strategy* and *trigger optimization mechanism*. Each malicious client c^* executes PPS and TOM to generate poisoned prototypes P_{c^*} and optimize label-specific triggers, respectively. Specifically, the poisoned prototypes of PPS deliberately bias the global prototypes away from the trigger prototypes. This manipulation indirectly influences the prototype learning of benign clients, pushing their benign prototypes to diverge from the trigger prototypes. As this discrepancy increases, trigger-embedded samples are more likely to be misclassified by benign models. Meanwhile, TOM expands the target label space and optimizes triggers for each target label. This increases the probability that the target

labels overlap with the local label space of benign clients, thereby enabling the benign models to inadvertently activate the *trigger-target label* mapping. Further theoretical analysis of BAPFL is provided in Appendix A.

Prototype Poisoning Strategy (PPS)

PPS includes two steps: sample selection and prototype flipping. The former identifies the most valuable trigger-embedded samples. The prototypes of these selected samples serve as the basis for the latter, which constructs the accurate poisoned prototypes in a deliberately opposite direction, thereby manipulating the global prototypes away from the trigger prototypes.

Sample Selection Strategy Malicious clients first compute the attack value of each trigger-embedded sample x^* by computing the Euclidean distance between its prototype $\phi(x^*)$ and the global prototype $\bar{P}^{(y)}$, where y is the ground-truth label of the clean sample x related to x^* . That is,

$$V(x^*) = \|\phi(x^*) - \bar{P}^{(y)}\|_2, \quad (6)$$

where a larger distance implies higher attack value. The top- K samples with the highest attack values are selected for training local model and constructing poisoned prototypes.

Prototype Flipping Strategy To mislead the global prototype, malicious clients construct poisoned prototypes and upload them to the server. Specifically, malicious client c^* first computes the class-wise trigger prototype $P_{tr}^{(k)}$ from the selected samples. Then, c^* computes the projection of $P_{tr}^{(k)}$ onto the corresponding global prototype $\bar{P}^{(k)}$. Finally, c^* constructs the poisoned prototype $P_{c^*}^{(k)}$ by performing a symmetrical flip of $P_{tr}^{(k)}$ with respect to this projection, i.e.,

$$P_{c^*}^{(k)} = 2 \cdot P_{proj} - P_{tr}^{(k)}, \quad (7)$$

where $P_{proj} = \frac{\bar{P}^{(k)} \cdot P_{tr}^{(k)}}{\bar{P}^{(k)} \cdot \bar{P}^{(k)}} \cdot \bar{P}^{(k)}$ denotes the projection of $P_{tr}^{(k)}$ onto $\bar{P}^{(k)}$. Compared with other flipping strategies such as origin-based or global prototype-based symmetry, our proposed prototype flipping strategy achieves finer control over both the direction and the norm of poisoned prototypes (see Appendix B). This ensures both effective and stealthy manipulation of benign clients' prototype learning.

Trigger Optimization Mechanism (TOM)

TOM includes two steps: trigger optimization and trigger training. The former designates a specific trigger to each target label, while the latter trains these triggers to achieve optimal effectiveness and stealthiness.

Trigger Optimization Strategy To enhance attack effectiveness across benign clients with heterogeneous data, we expand the attack's target label space from a single label y_t to a label set Y_t that encompasses all local labels of benign clients. For each target label $y_t \in Y_t$, a specific trigger (δ_{y_t}, M_{y_t}) is learned. This design enables BAPFL to perform personalized backdoor attacks on benign clients.

Algorithm 1 PFL process with BAPFL Attack

- 1: **Server Executes:**
 - 2: Initialize global prototypes $\bar{P} = \{\bar{P}^{(k)}\}_{k=1,2,\dots}$
 - 3: **while** the current training round \leq the final round **do**
 - 4: Broadcast \bar{P} to clients for local training
 - 5: Aggregate the local prototypes of clients to update \bar{P}
 - 6: **end while**
 - 7: **Client Executes:**
 - 8: **if** this client is compromised **then**
 - 9: */*Execute TOM*/*
 - 10: Triggers \leftarrow Download the trigger network from the adversary and train it with \bar{P} based on Equation (8)
 - 11: */*Execute PPS*/*
 - 12: Select the top- K samples with the highest attack value based on Equation (6)
 - 13: Train f_θ according to Equation (5)
 - 14: Poisoned prototypes $P_c \leftarrow$ Flip trigger prototypes
 - 15: **else**
 - 16: Train P_c and f_θ with \bar{P} according to Equation (4)
 - 17: **end if**
 - 18: **return** the new prototypes P_c to the server
-

Dataset	Labels	Image size	Training /Test images	Model
MNIST	10	1*28*28	60k/10k	2Conv + 2Fc
FEMNIST	10	1*128*128	22k/3k	2Conv + 2Fc
CIFAR-10	10	3*32*32	50k/10k	2Conv + Pool + 3Fc

Table 1: Dataset and model architecture

Specifically, if the local label space of benign client c contains the target label y_t , BAPFL can activate backdoor behaviors of c 's local model, enabling it to classify the samples embedded with the trigger (δ_{y_t}, M_{y_t}) as y_t .

Trigger Training Strategy For each target label y_t , we learn a dedicated trigger pattern δ_{y_t} and a corresponding mask M_{y_t} , forming a trigger function $T_{y_t}(x) = (1 - M_{y_t}) \odot x + M_{y_t} \odot \delta_{y_t}$. The optimization objective of each trigger aims to simultaneously: 1) minimize classification loss of $T_{y_t}(x)$ to y_t , 2) align the prototype of $T_{y_t}(x)$ with the global prototype $\bar{P}^{(y_t)}$, and 3) ensure visual imperceptibility of the trigger. The corresponding loss function is formulated as:

$$\mathcal{L}_{trigger} = \underbrace{\mathcal{L}_S(f_\theta(T_{y_t}(x)), y_t)}_{\text{target classification loss}} + \lambda_1 \cdot \underbrace{\|\phi(T_{y_t}(x)) - \bar{P}^{(y_t)}\|_2}_{\text{prototype alignment}} + \lambda_2 \cdot \underbrace{\|M_{y_t}\|_1 + \lambda_3 \cdot \|\delta_{y_t}\|_2}_{\text{stealthiness loss}}, \quad (8)$$

where λ_1 , λ_2 , and λ_3 are hyperparameters controlling the trade-off between effectiveness and stealthiness.

Performance Evaluation

Experiment Setup

Datasets and Models Our experiments are conducted on three datasets: MNIST (LeCun, Cortes, and Burges 1998),

Method	AR = 10%		AR = 20%		AR = 30%		AR = 40%	
	ACC	ASR	ACC	ASR	ACC	ASR	ACC	ASR
MNIST								
MR	96.79	13.29	97.39	24.54	97.47	40.27	97.89	50.99
DBA	97.60	38.52	97.51	42.44	96.04	49.94	98.08	56.40
BAPFL	97.96	87.14	97.85	88.38	96.89	88.89	96.90	91.08
FEMNIST								
MR	90.97	13.68	91.31	34.18	90.17	18.73	88.31	28.52
DBA	89.80	11.71	91.21	17.96	89.83	21.10	89.41	41.67
BAPFL	91.94	87.39	91.29	88.48	90.55	89.19	89.18	89.23
CIFAR-10								
MR	66.10	11.32	63.93	13.08	60.75	13.36	66.31	13.81
DBA	65.97	10.25	60.31	10.63	65.71	13.48	66.44	13.59
BAPFL	62.38	77.38	61.47	77.78	60.93	78.20	60.83	82.00

Table 2: ACC and ASR of BAPFL and baselines in PFL.

FEMNIST (Caldas et al. 2019), and CIFAR-10 (Krizhevsky 2009), which are benchmark datasets for image classification. The dataset and model details are provided in Table 1.

Training Setting In our experiments, we choose FedProto (Tan et al. 2022a) as the basic PFL framework. The number of clients is set to 20 and the total training rounds are set to 200. In each training round, each client performs 1 local epoch with a local batch size of 4, and the learning rate is set to 0.01. We assume that all clients perform learning tasks with heterogeneous statistical distributions. Specifically, each client is assigned a p -way q -shot classification task, where p and q denote the number of local classes and the number of samples per class, respectively. We also introduce a standard deviation std to p and q to achieve enhanced heterogeneity for different clients. By default, we set $p = 5$, $q = 100$, and $std = 2$. Additionally, we set $\alpha = 0.75$, $\lambda = 1$, $\lambda_1 = 0.1$, $\lambda_2 = 0.01$ and $\lambda_3 = 0.001$. All experiments are repeated 10 times, and the average results are reported.

Baselines To evaluate the effectiveness of BAPFL, we compare it with two representative backdoor attack baselines: MR and DBA. We also assess the adaptability of BAPFL across other PFL frameworks, including FedPD (Tan et al. 2025) and FedPCL (Tan et al. 2022b).

Attack Setup We simulate a backdoor attack scenario where the attacker controls 10%, 20%, 30%, or 40% of the clients. For each ground-truth label y , the target label is set to $9 - y$. The compromised clients train triggers for their target labels over 50 local rounds and embed them into their local data to construct poisoned prototypes. During the training process of compromised clients, we set the trigger and the local model to be trained alternately.

Evaluation Metrics We report the average main task accuracy (ACC, %) over clean samples and average attack success rate (ASR, %) over trigger-embedded samples for all benign clients’ models on their test datasets.

Method	AR = 10%		AR = 20%		AR = 30%		AR = 40%	
	ACC	ASR	ACC	ASR	ACC	ASR	ACC	ASR
FedPCL	49.11	72.91	48.64	75.89	48.61	78.78	49.81	81.82
FedPD	97.87	65.11	97.91	70.56	96.97	77.74	97.28	79.40

Table 3: BAPFL performance in various PFL frameworks.

Main Results

Comparisons Between BAPFL and Baselines In the PFL framework FedProto, we compare the performance of BAPFL with baselines, i.e., MR and DBA, under varying attack rates (AR) on MNIST, FEMNIST, and CIFAR-10. As shown in Table 2, BAPFL consistently achieves the highest ASR across all settings, while maintaining comparable or even higher ACC. Notably, BAPFL improves ASR by 35%–75% over MR and DBA, demonstrating its superior effectiveness and stealthiness in PFL.

Integrate BAPFL into Different PFL Frameworks To demonstrate the adaptability of BAPFL, we evaluate its effectiveness against two other representative PFL frameworks: FedPCL and FedPD. FedPCL employs a contrastive loss to enhance prototype alignment. FedPD adopts robust aggregation based on cosine similarity and encourages inter-class prototype separation. We apply BAPFL to FedPCL on the OFFICE-10 dataset (Gong et al. 2012), and to FedPD on MNIST, respectively. The results are shown in Table 3. We observe that as the attack rate increases, the ASR of BAPFL in FedPCL increases from 72.91% to 81.82%, while ACC remains stable. This confirms the vulnerability of FedPCL to our attack. Moreover, although FedPD adopts robust aggregation, BAPFL still achieves 65.11%–79.4% ASR, demonstrating its ability to bypass FedPD’s defense.

Data Heterogeneity To evaluate the robustness of BAPFL under varying degrees of data heterogeneity, we simulate different data heterogeneity scenarios by adjusting the values of p , q , and std across clients. Specifically, for MNIST, we fix $q = 100$, $std = 2$, and vary p from 3 to 7. For FEMNIST, we fix $p = 5$, $std = 2$, and vary q from 40 to 120. For CIFAR-10, we fix $p = 5$, $q = 100$, and vary std from 1 to 5. Then, we evaluate the ASR of our BAPFL method under these settings. The experimental results in Figure 6 show that BAPFL consistently achieves ASR of at least 75% across all heterogeneous settings, demonstrating its strong robustness.

The Effect of λ for BAPFL To assess the effect of the weight λ of \mathcal{L}_P for BAPFL, we evaluate the ASR and ACC of BAPFL in PFL with $\lambda \in \{1, 2, 3, 4, 5\}$. Figure 7 presents the experimental results on the MNIST dataset. We observe that BAPFL achieves consistently high ASR across all settings, with only minor fluctuations across different λ values. Moreover, the ACC of BAPFL generally remains stable. However, under high attack rates, the ACC of BAPFL decreases slightly as λ increases. For example, when the attack rate is 40%, the ACC value drops from 97% ($\lambda = 1$) to 92% ($\lambda = 5$). The attacker can mitigate this effect by reducing the attack rate. Overall, BAPFL demonstrates its

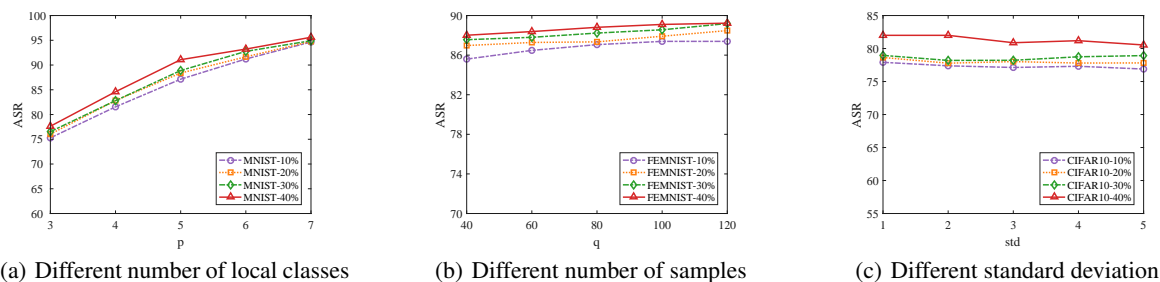


Figure 6: The ASR of BAPFL under varying degrees of data heterogeneity.

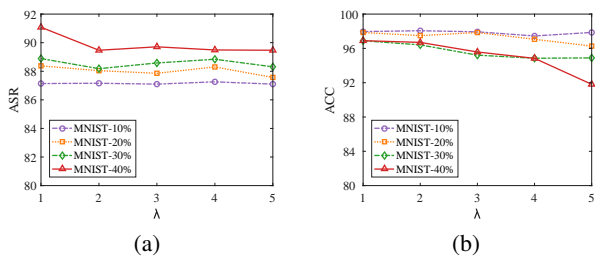


Figure 7: Effect of the weight λ on ASR and ACC of BAPFL on the MNIST dataset.

Method	AR = 10%		AR = 20%		AR = 30%		AR = 40%	
	ACC	ASR	ACC	ASR	ACC	ASR	ACC	ASR
MNIST								
DBA	97.60	38.52	97.51	42.44	96.04	49.94	98.08	56.40
DBA+PPS	98.05	62.15	97.98	69.43	97.72	71.50	97.48	75.64
PPS+TOM	97.96	87.14	97.85	88.38	96.89	88.89	96.90	91.08
FEMNIST								
DBA	89.80	11.71	91.21	17.96	89.83	21.10	89.41	41.67
DBA+PPS	89.80	60.25	90.09	69.72	89.72	72.72	88.91	73.58
PPS+TOM	91.94	87.39	91.29	88.48	90.55	89.19	89.18	89.23
CIFAR-10								
DBA	65.97	10.25	60.31	10.63	65.71	13.48	66.44	13.59
DBA+PPS	65.59	45.64	61.86	47.85	61.87	49.93	65.16	50.69
PPS+TOM	62.38	77.38	61.47	77.78	60.93	78.20	60.83	82.00

Table 4: Ablation results of BAPFL on MNIST, FEMNIST, and CIFAR-10 datasets under different attack rates.

effectiveness under different λ settings.

Ablation Study

Effectiveness of BAPFL Components To evaluate the effectiveness of each component in BAPFL, we conduct an ablation study of BAPFL on three datasets, i.e., MNIST, FEMNIST, and CIFAR-10. Specifically, we examine the individual contributions of the PPS and TOM in BAPFL. The experimental results under different datasets and various attack rates are summarized in Table 4. Across all datasets, BAPFL(PPS+TOM) consistently achieves the highest ASR with minimal impact on ACC. Removing either component significantly reduces ASR of BAPFL.

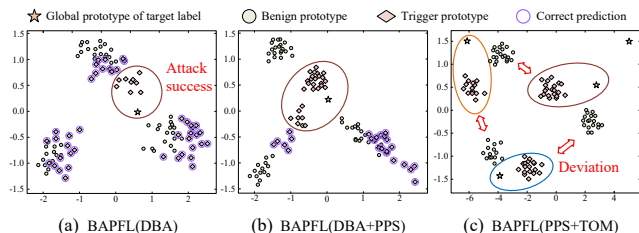


Figure 8: The principal component analysis (PCA) visualization of benign and trigger prototypes for benign client 1 under different attack strategies. The trigger prototypes classified as the original label are marked with purple circles.

For example, in the ablation study based on MNIST, when AR is 20%, BAPFL(PPS+TOM) achieves 88.38% ASR, while BAPFL(DBA+PPS) drops ASR to 69.43%, and BAPFL(DBA) alone achieves only 42.44%. Similar trends are observed in results based on FEMNIST and CIFAR-10. These results highlight that both PPS and TOM are essential for enhancing BAPFL’s effectiveness.

Case Study To further illustrate the effectiveness of the PPS and TOM of BAPFL, we conduct a case study on FEMNIST, in which we visualize the prototype distribution and the classification results of trigger prototypes for a benign client under three attack strategies: BAPFL(DBA), BAPFL(DBA+PPS), and BAPFL(PPS+TOM). As shown in Figure 8(a), the trigger prototypes of BAPFL(DBA) are optimized toward the global prototype of the target label, but most of them are still close to their corresponding benign prototypes. This leads to a low ASR. In contrast, in the case of BAPFL(DBA+PPS) (Figure 8(b)), PPS separates the benign prototypes from the trigger prototypes. This enables more trigger prototypes to approach the global prototype of the target label, which increases the ASR. Finally, in the case of BAPFL(PPS+TOM) (Figure 8(c)), TOM further expands the target label space and enhances the alignment of trigger prototypes with the global prototype of the target labels, achieving the highest ASR across all attack strategies. The above results indicate that both PPS and TOM in BAPFL play a crucial role in enhancing the ASR.

Conclusions and Future Work

In this paper, we investigate the problems of applying existing backdoor attacks in PFL and propose a novel and effective backdoor attack method BAPFL. By carefully designing poisoned prototypes and optimizing specific triggers for target labels, BAPFL successfully induces targeted misclassifications in benign models while evading detection. Comprehensive evaluations across diverse datasets and PFL frameworks demonstrate that BAPFL significantly improves ASR with negligible performance degradation on main tasks. BAPFL underscores the need for stronger defenses in PFL and provides insights into designing secure and trustworthy PFL systems. In future work, we intend to extend our methodology to other FL frameworks that adopt non-gradient-based aggregation strategies.

References

- Bagdasaryan, E.; Veit, A.; Hua, Y.; Estrin, D.; and Shmatikov, V. 2020. How To Backdoor Federated Learning. In *Proceedings of the Twenty Third International Conference on Artificial Intelligence and Statistics*, 2938–2948.
- Caldas, S.; Duddu, S. M. K.; Wu, P.; Li, T.; Konečný, J.; McMahan, H. B.; Smith, V.; and Talwalkar, A. 2019. LEAF: A Benchmark for Federated Settings. arXiv:1812.01097.
- Chen, Z.; Yu, S.; Chen, F.; Wang, F.; Liu, X.; and Deng, R. H. 2024. Lightweight Privacy-Preserving Cross-Cluster Federated Learning With Heterogeneous Data. *IEEE Transactions on Information Forensics and Security*, 19(19): 7404–7419.
- Fan, M.; Hu, Z.; Wang, F.; and Chen, C. 2025. Bad-PFL: Exploring Backdoor Attacks against Personalized Federated Learning. In *Proceedings of the International Conference on Learning Representations (ICLR'25)*.
- Feng, J.; Lai, Y.; Sun, H.; and Ren, B. 2025. SADBA: Self-Adaptive Distributed Backdoor Attack Against Federated Learning. In *Proceedings of the Thirty-Ninth AAAI Conference on Artificial Intelligence (AAAI'25)*, 16568–16576.
- Fu, C.; Zhang, X.; Ji, S.; Chen, J.; Wu, J.; Guo, S.; Zhou, J.; Liu, A. X.; and Wang, T. 2022. Label Inference Attacks Against Vertical Federated Learning. In *31st USENIX Security Symposium (USENIX Security 22)*, 1397–1414.
- Fu, L.; Huang, S.; Lai, Y.; Liao, T.; Zhang, C.; and Chen, C. 2025a. Beyond Federated Prototype Learning: Learnable Semantic Anchors with Hyperspherical Contrast for Domain-Skewed Data. In *Proceedings of the AAAI Conference on Artificial Intelligence (AAAI'25)*, 16648–16656.
- Fu, L.; Huang, S.; Lai, Y.; Liao, T.; Zhang, C.; and Chen, C. 2025b. Beyond Federated Prototype Learning: Learnable Semantic Anchors with Hyperspherical Contrast for Domain-Skewed Data. In *Proceedings of the AAAI Conference on Artificial Intelligence (AAAI'25)*, 16648–16656.
- Gong, B.; Shi, Y.; Sha, F.; and Grauman, K. 2012. Geodesic Flow Kernel for Unsupervised Domain Adaptation. In *Proceedings of the 2012 IEEE Conference on Computer Vision and Pattern Recognition (CVPR'12)*, 2066–2073.
- Huang, W.; Ye, M.; Shi, Z.; Li, H.; and Du, B. 2023a. Rethinking Federated Learning With Domain Shift: A Prototype View. In *Proceedings of the IEEE/CVF Conference on Computer Vision and Pattern Recognition (CVPR'23)*, 16312–16322.
- Huang, W.; Ye, M.; Shi, Z.; Li, H.; and Du, B. 2023b. Rethinking Federated Learning with Domain Shift: A Prototype View. In *2023 IEEE/CVF Conference on Computer Vision and Pattern Recognition (CVPR'23)*, 16312–16322.
- Jiang, L.; Wang, X.; Yang, X.; Shu, J.; Lin, H.; and Yi, X. 2025. FedPA: Generator-Based Heterogeneous Federated Prototype Adversarial Learning. *IEEE Transactions on Dependable and Secure Computing*, 22(2): 939–949.
- Krizhevsky, A. 2009. Learning Multiple Layers of Features from Tiny Images. <https://www.cs.toronto.edu/~kriz/cifar.html>. Accessed: 2025-06-15.
- LeCun, Y.; Cortes, C.; and Burges, C. J. 1998. The MNIST Database. <http://yann.lecun.com/exdb/mnist/>. Accessed: 2025-06-15.
- Li, H.; Ye, Q.; Hu, H.; Li, J.; Wang, L.; Fang, C.; and Shi, J. 2023. 3DFed: Adaptive and Extensible Framework for Covert Backdoor Attack in Federated Learning. In *Proceedings of the 2023 IEEE Symposium on Security and Privacy (SP'23)*, 1893–1907.
- Li, T.; Sahu, A. K.; Zaheer, M.; Sanjabi, M.; Talwalkar, A.; and Smith, V. 2020. Federated Optimization in Heterogeneous Networks. In *Proceedings of the 3rd Conference on Machine Learning and Systems (MLSys'20)*, 429–450.
- Li, Y.; Tao, X.; Zhang, X.; Liu, J.; and Xu, J. 2022. Privacy-Preserved Federated Learning for Autonomous Driving. *IEEE Transactions on Intelligent Transportation Systems*, 23(7): 8423–8434.
- Liu, T.; Zhang, Y.; Feng, Z.; Yang, Z.; Xu, C.; Man, D.; and Yang, W. 2024. Beyond Traditional Threats: A Persistent Backdoor Attack on Federated Learning. In *Proceedings of the AAAI Conference on Artificial Intelligence (AAAI'24)*, 21359–21367.
- Liu, Z.; Chen, Y.; Zhao, Y.; Yu, H.; Liu, Y.; Bao, R.; Jiang, J.; Nie, Z.; Xu, Q.; and Yang, Q. 2022. Contribution-Aware Federated Learning for Smart Healthcare. In *Proceedings of the AAAI Conference on Artificial Intelligence (AAAI'22)*, 12396–12404.
- Lyu, X.; Han, Y.; Wang, W.; Liu, J.; Zhu, Y.; Xu, G.; Liu, J.; and Zhang, X. 2024. Lurking in the shadows: unveiling stealthy backdoor attacks against personalized federated learning. In *Proceedings of the 33rd USENIX Conference on Security Symposium (USENIX Security'24)*, 18.
- Mu, X.; Shen, Y.; Cheng, K.; Geng, X.; Fu, J.; Zhang, T.; and Zhang, Z. 2023. FedProc: Prototypical contrastive federated learning on non-IID data. *Future Generation Computer Systems*, 143(1): 93–104.
- Qin, Z.; Chen, F.; Zhi, C.; Yan, X.; and Deng, S. 2024. Resisting Backdoor Attacks in Federated Learning via Bidirectional Elections and Individual Perspective. In *Proceedings of the AAAI Conference on Artificial Intelligence (AAAI'24)*, 14677–14685.

Tan, Y.; Long, G.; Liu, L.; Zhou, T.; Lu, Q.; Jiang, J.; and Zhang, C. 2022a. FedProto: Federated Prototype Learning across Heterogeneous Clients. In *Proceedings of the Thirty-Sixth AAAI Conference on Artificial Intelligence (AAAI'22)*, 8432–8440.

Tan, Y.; Long, G.; Ma, J.; LIU, L.; Zhou, T.; and Jiang, J. 2022b. Federated Learning from Pre-Trained Models: A Contrastive Learning Approach. In *Advances in Neural Information Processing Systems (NeurIPS'22)*, 19332–19344.

Tan, Z.; Cai, J.; Li, D.; Lian, P.; Liu, X.; and Che, Y. 2025. FedPD: Defending Federated Prototype Learning against Backdoor Attacks. *Neural Networks*, 184(C): 107016.

Wang, L.; Bian, J.; Zhang, L.; Chen, C.; and Xu, J. 2024. Taming Cross-Domain Representation Variance in Federated Prototype Learning with Heterogeneous Data Domains. In *Advances in Neural Information Processing Systems (NeurIPS'24)*, 88348–88372.

Wen, H.; Wu, Y.; Hu, J.; Wang, Z.; Duan, H.; and Min, G. 2023. Communication-Efficient Federated Learning on Non-IID Data Using Two-Step Knowledge Distillation. *IEEE Internet of Things Journal*, 10(19): 17307–17322.

Xie, C.; Huang, K.; Chen, P.-Y.; and Li, B. 2020. DBA: Distributed Backdoor Attacks against Federated Learning. In *International Conference on Learning Representations (ICLR'20)*.

Yan, B.; Zhang, H.; Xu, M.; Yu, D.; and Cheng, X. 2024. FedRFQ: Prototype-Based Federated Learning With Reduced Redundancy, Minimal Failure, and Enhanced Quality. *IEEE Transactions on Computers*, 73(4): 1086–1098.

Ye, T.; Chen, C.; Wang, Y.; Li, X.; and Gao, M. 2024. BapFL: You can Backdoor Personalized Federated Learning. *ACM Transactions on Knowledge Discovery from Data*, 18(7): 166.

Zhang, C.; Long, G.; Zhou, T.; Zhang, Z.; Yan, P.; and Yang, B. 2024. Gpfedrec: Graph-guided personalization for federated recommendation. In *Proceedings of the 30th ACM SIGKDD Conference on Knowledge Discovery and Data Mining (KDD'24)*, 4131–4142.

Zhang, H.; Li, C.; Dai, W.; Zou, J.; and Xiong, H. 2023a. FedCR: Personalized Federated Learning Based on Across-Client Common Representation with Conditional Mutual Information Regularization. In *Proceedings of the 40th International Conference on Machine Learning (ICML'23)*, 41314–41330.

Zhang, J.; Hua, Y.; Wang, H.; Song, T.; Xue, Z.; Ma, R.; Cao, J.; and Guan, H. 2023b. GPFL: Simultaneously Learning Global and Personalized Feature Information for Personalized Federated Learning. In *2023 IEEE/CVF International Conference on Computer Vision (ICCV'23)*, 5018–5028.

Zhang, J.; Hua, Y.; Wang, H.; Song, T.; Xue, Z.; Ma, R.; and Guan, H. 2023c. FedALA: Adaptive Local Aggregation for Personalized Federated Learning. In *Proceedings of the AAAI Conference on Artificial Intelligence (AAAI'23)*, 11237–11244.

Zhou, Y.; Pang, X.; Wang, Z.; Hu, J.; Sun, P.; and Ren, K. 2024. Towards Efficient Asynchronous Federated Learn-

ing in Heterogeneous Edge Environments. In *IEEE INFOCOM 2024 - IEEE Conference on Computer Communications*, 2448–2457.

Appendix A: Theoretical Analysis of BAPFL

In this appendix, we formally analyze how the proposed BAPFL enhances backdoor effectiveness in prototype-based federated learning (PFL).

Effectiveness of PPS

We first introduce a key assumption that underlies prototype-based classification in PFL.

Assumption 1. In a well-trained PFL model, a sample x is classified as label k if its extracted feature $\phi(x)$ is closer (in ℓ_2 distance) to the global prototype $\bar{P}^{(k)}$ than to any other prototype. That is,

$$\text{label}(x) = \arg \min_k \|\phi(x) - \bar{P}^{(k)}\|_2.$$

Under this assumption, the attack success rate (ASR) is increased if the features of trigger-embedded samples $\phi(T_{y_t}(x))$ are misaligned with the global prototype $\bar{P}^{(y)}$ of the original label and become closer to other class prototypes. We now show that PPS increases this misalignment by manipulating the process of prototype aggregation.

Theorem 1. The PPS increases the misclassification probability of trigger-embedded samples in benign models by poisoning the global prototype aggregation. Specifically, it manipulates the global prototype $\bar{P}^{(k)}$ of class k to deviate from the trigger prototype $P_{tr}^{(k)}$, thereby misleading the optimization of benign prototypes and increasing the distance between the benign prototype $P_c^{(k)}$ and $P_{tr}^{(k)}$.

Proof: $\bar{P}^{(k)}$ is computed as the average of clients' local prototypes, i.e.,

$$\bar{P}^{(k)} = \frac{1}{C} \sum_{c=1}^C P_c^{(k)}.$$

The malicious client c^* uploads a poisoned prototype $P_{c^*}^{(k)}$ defined as:

$$P_{c^*}^{(k)} = 2 \cdot P_{proj} - P_{tr}^{(k)},$$

where

$$P_{proj} = \frac{\bar{P}^{(k)} \cdot P_{tr}^{(k)}}{P^{(k)} \cdot \bar{P}^{(k)}} \cdot \bar{P}^{(k)}.$$

This poisoned prototype $P_{c^*}^{(k)}$ is the reflection of $P_{tr}^{(k)}$ with respect to the projection point P_{proj} on $\bar{P}^{(k)}$, thus intentionally pushing the aggregated prototype away from the direction of $P_{tr}^{(k)}$. Let C_b denote the set of benign clients and C_m the set of malicious clients. The new aggregated global prototype becomes:

$$\bar{P}_{\text{new}}^{(k)} = \frac{1}{|C_b| + |C_m|} \left(\sum_{c \in C_b} P_c^{(k)} + \sum_{c^* \in C_m} P_{c^*}^{(k)} \right).$$

Since the poisoned prototypes are reflected points away from $P_{tr}^{(k)}$, the vector $\bar{P}_{new}^{(k)} - P_{tr}^{(k)}$ increases in magnitude compared to $\bar{P}^{(k)} - P_{tr}^{(k)}$, i.e.,

$$\|\bar{P}_{new}^{(k)} - P_{tr}^{(k)}\|_2 > \|\bar{P}^{(k)} - P_{tr}^{(k)}\|_2.$$

In the subsequent training rounds, benign clients optimize their local prototypes $P_c^{(k)}$ to minimize the consistency loss \mathcal{L}_P with the (now biased) global prototype:

$$\mathcal{L}_P = \|P_c^{(k)} - \bar{P}_{new}^{(k)}\|_2.$$

Thus, $P_c^{(k)}$ is continuously pulled toward $\bar{P}_{new}^{(k)}$, and consequently, $\|P_c^{(k)} - P_{tr}^{(k)}\|_2$ increases over training rounds. According to *Assumption 1*, for a clean sample x , if its feature $\phi(x)$ approximates $P_c^{(k)}$, then the classification result of this sample x is:

$$k = \arg \min_j \|\phi(x) - \bar{P}_{new}^{(j)}\|_2.$$

For the corresponding trigger-embedded sample x^* with target label y_t , its feature $\phi(x^*)$ approximates $P_{tr}^{(k)}$. Since $\|P_c^{(k)} - P_{tr}^{(k)}\|$ becomes larger due to PPS, the probability that $\phi(x^*)$ is closest to $\bar{P}_{new}^{(k)}$ decreases, i.e.,

$$\Pr \left[\arg \min_j \|\phi(x^*) - \bar{P}_{new}^{(j)}\|_2 = k \right] \downarrow.$$

Therefore, PPS increases the misclassification probability of trigger-embedded samples in benign models.

Effectiveness of TOM

We now analyze how TOM increases the ASR in PFL. Specifically, by aligning trigger prototypes with the global prototypes of target labels that overlap with local label spaces, TOM increases the probability that the trigger-target label mapping is unintentionally activated in benign clients.

Assumption 2. For a trigger-embedded sample x^* with target label y_t , its classification is determined by the proximity of its feature $\phi(T_{y_t}(x))$ to the global prototype $\bar{P}^{(k)}$:

$$\text{label}(T_{y_t}(x)) = \arg \min_k \|\phi(T_{y_t}(x)) - \bar{P}^{(k)}\|_2.$$

Theorem 2. TOM increases the probability that the trigger-target label mapping is unintentionally activated by benign models.

Proof: Let Y_t denote the set of target labels chosen by the attacker, where:

$$Y_t = \bigcup_{c \in C_b} \mathcal{Y}_c,$$

and \mathcal{Y}_c is the local label space of benign client c . Y_t maximizes the probability that any benign client c has $y_t \in \mathcal{Y}_c$ for some $y_t \in Y_t$. For each target label $y_t \in Y_t$, TOM optimizes a dedicated trigger pattern (δ_{y_t}, M_{y_t}) to construct a trigger function:

$$T_{y_t}(x) = (1 - M_{y_t}) \odot x + M_{y_t} \odot \delta_{y_t}.$$

TOM jointly optimizes (δ_{y_t}, M_{y_t}) to minimize the loss $\mathcal{L}_{\text{trigger}}$. After training, $P_{tr}^{(y_t)} \approx \bar{P}^{(y_t)}$. Now consider a

Strategy	10%		20%		30%		40%	
	ACC	ASR	ACC	ASR	ACC	ASR	ACC	ASR
MNIST								
OBF	98.10	87.10	97.52	87.58	96.67	88.18	96.79	89.40
GPF	97.71	77.18	98.15	83.23	98.21	85.67	98.01	87.57
PFS	97.96	87.14	97.85	88.38	96.89	88.89	96.90	91.08
FEMNIST								
OBF	91.69	83.45	91.62	85.36	90.49	86.60	89.90	87.56
GPF	91.11	81.88	91.06	83.02	89.93	84.23	89.56	85.82
PFS	91.94	87.39	91.29	88.48	90.55	89.19	89.18	89.23
CIFAR-10								
OBF	62.21	73.04	60.23	73.19	58.57	73.21	64.67	73.43
GPF	63.54	72.86	61.45	73.33	58.36	73.48	61.06	73.56
PFS	62.38	77.38	61.47	77.78	60.93	78.20	60.83	82.00

Table 5: Performance comparison of BAFPL with different flipping strategies.

benign client c such that $y_t \in \mathcal{Y}_c$. Suppose the trigger-embedded sample $T_{y_t}(x)$ is injected into c 's testing batch, TOM increases the likelihood that:

$$\phi(T_{y_t}(x)) \approx P_{tr}^{(y_t)} \approx \bar{P}^{(y_t)}.$$

Therefore, under *Assumption 2*, the probability that a benign model classifies $T_{y_t}(x)$ as y_t increases:

$$\Pr \left[\arg \min_k \|\phi(T_{y_t}(x)) - \bar{P}^{(k)}\|_2 = y_t \right] \uparrow.$$

Hence, TOM increases the chance of ‘‘unintentional backdoor activation’’ across benign clients.

In conclusion, our theoretical analysis demonstrates that the integration of PPS and TOM enables BAPFL to effectively enhance the the ASR in PFL.

Appendix B: Comparison of Different Flipping Strategies

To validate the effectiveness of our proposed prototype flipping strategy (PFS) in the PPS, we compare it against two intuitive baselines: 1) *Origin-based flipping (OBF)*. This strategy reflects the trigger prototype $P_{tr}^{(k)}$ based on the origin to construct the poisoned prototype $P_{c^*}^{(k)}$, i.e.,

$$P_{c^*}^{(k)} = -P_{tr}^{(k)}.$$

Although simple and effective, OBF reduces the stealthiness of the attack since it often yields unstable or easily detectable poisoned prototypes that are significantly different from the benign prototypes. 2) *Global prototype-based flipping (GPF)*. This strategy reflects $P_{tr}^{(k)}$ with respect to the global prototype $\bar{P}^{(k)}$ to construct $P_{c^*}^{(k)}$, i.e.,

$$P_{c^*}^{(k)} = 2 \cdot \bar{P}^{(k)} - P_{tr}^{(k)}.$$

Compared with OBF, GPF achieves finer control over the direction of $P_{c^*}^{(k)}$, but it lacks control over the norm of $P_{c^*}^{(k)}$, potentially weakening attack effectiveness or introducing excessive perturbation.

Conversely, our PFS enables fine-grained control over both the direction and norm of $P_{c^*}^{(k)}$, achieving more precise manipulation of the global prototype while preserving stealth.

Experimental Comparison. In PFL, we report the main task accuracy (ACC) and ASR of BAPFL with different flipping strategies across three datasets (MNIST, FEMNIST, CIFAR-10) and varying attack rates (AR = 10% to 40%). The results are shown in Table 5. Across all datasets and attack rates, the BAPFL with PFS consistently achieves the highest ASR while maintaining comparable or even better ACC than other baselines. This demonstrates that our strategy provides a more effective and stealthy attack mechanism by precisely constructing the direction and norm of the poisoned prototypes.